Indonesian Journal of Aerospace Vol. 22 No. 1 Juni 2024 : pp 57 – 70 (Birry et al.)
DOI: 10.59981/ijoa.2024.2784
https://ejournal.brin.go.id/ijoa/

Evaluation of Artificial Neural Networks Technique for Calibration of Five-Hole Probe Measurement

Abdurrahman Birry [1,2], Ony Arifianto [2], Taufiq Mulyanto [2]

[1]Test Instrumentation System, Indonesian Aerospace, Indonesia
[2]Faculty of Mechanical and Aerospace Engineering, Institut Teknologi Bandung, Indonesia
e-mail: 23621305@mahasiswa.itb.ac.id

Received: 30-09-2023. Accepted: 27-09-2024. Published: 31-12-2024

Abstract

In the present study, the Artificial Neural Networks (ANN) technique was implemented to predict the flow parameters of a Five-Hole Probe (FHP). The experimental data were obtained from a subsonic open jet wind tunnel at a speed increased from 0 to 1180 rpm in increments of 200 rpm. The ANN approach is carried out in stages, starting with the method of selecting training data and validation, then increasing the number of neurons, varying the correlation between the activation function and the optimizer, and finally finding the optimal number of hidden layers. In the ANN approach, the mean absolute errors of 0.2705, 0.3326, and 1.0748 were achieved for estimating angle α which represents the angle of attack, angle β which represents the angle of sideslip, and speed, respectively. At the end of this study, the results were compared with the rational function approach. It was concluded that the ANN approach was more accurate compared to the rational function based on statistical parameters such as mean absolute error, max absolute error, and coefficient of determination (r^2).

Keywords**:** *five-hole probe, artificial neural network, calibration, wind tunnel, rational function.*

Nomenclature

α	=	Angle of Attack, degree
β	=	Angle of Sideslip, degree
r^2	=	Coefficient of determinations

1. Introduction

Angles of Attack (AoA), Angles of Sideslip (AoS), and airspeed (V) are critical parameters essential for enhancing the stability and controllability of aircraft, particularly during take-off and landing. Numerous research efforts, as exemplified by Popowski & Dabrowski. (2015) and more recently Liu. (2023), have investigated estimation methods for these angles. Popowski & Dabrowski. (2015) employed estimates based on measuring linear velocity components of an object in Earth's coordinates and on the object's attitude angles. Liu. (2023) introduced an estimation method based on the Air Data System (ADS), Inertial Navigation System (INS), and aircraft aerodynamic data. Flight test data analysis from these studies indicates that the angle of attack estimation error remains within 1°, and the side-slip angle estimation error is within 1.5°, meeting the requirements for engineering applications.

In addition to estimation methods, direct measurement methods for AoA and AoS often involve the use of pivoted vanes or pressure-type sensors, while airspeed measurements typically utilize pitot-static probes. However, the specificity of sensors for certain parameters necessitates the installation of numerous sensors on an aircraft.

The utilization of a pressure-type sensor, specifically a Multi-Hole Probe (MHP), offers an effective solution to reduce the number of sensors required on an aircraft. Multi-hole pressure probes serve as unique measurement instruments capable of simultaneously

measuring velocity components and pressure fields of the flow. Consequently, these probes can be employed to measure AoA, AoS, and airspeed. Another notable advantage of MHP lies in their lack of moving mechanical parts, rendering them more robust, and they do not necessitate recalibration as long as the probe remains unaltered or unaffected.

In this study, a novel approach will be employed for the calibration of Five-Hole Probe (FHP) pressure data. The proposed technique utilizes the Artificial Neural Network (ANN) approach to directly process the raw pressure data corresponding to angles α, β, and speed. The pressure data utilized in this research is sourced from the dataset presented by Arifianto and Farhood. (2015).

1. Methodology

1.1 Related Works

Many researchers utilize multi-hole probes including four-hole to eighteen-hole probes to measure air flow properties. The FHP was first used by Treaster & Yocum. (1978) as a pressure measuring tool in calculating velocity vectors and total and static pressures of the flow field. This technique encouraged researchers to use an FHP and to propose several techniques for FHP measurements. As did by Gallington. (1980), which uses a sectoring scheme that selects combinations of holes to which the flow is attached. Next, Ranjan Paul et al. (2011) defines a new pressure coefficient to overcome limitations in calculating flow parameters in the Gallington method. Then Pisasale & Ahmed. (2002) proposed a successful measurement technique that extended to an angle of 75°. Followed by Mortadha & Qureshi. (2019) for extending the usable range of the calibration map of a four-hole probe for measuring high flow angles. In their study, the researchers defined the non-dimensional pressure coefficient in different ways. The data reduction technique commonly used standard regression including linear interpolation and polynomial curve fit.

Recently, ANN has been used to calibrate FHP measurements. As in Nikpey Somehsaraei et al. (2020) which calibrates FHP measurements using a Multi-Layer Perceptron (MLP) network with 2 stages. The experimental data used are α and β angles in the range of ±25 degrees with a speed of Ma 0.1 to 0.8. The first stage determines the ANN model from the input which is the pressure coefficient from the α angle, β angle, and Ma number (namely, $k\alpha$, $k\beta$, kV, respectively) to the output in the form of α angle, β angle, and Ma number. In the second stage, determining the model from the prediction error results of the first stage is used as output to obtain an error prediction. Ultimately, the final prediction result is the sum of the stage 1 and stage 2 models. From the method above, it is known that this method outperforms the 5th-order polynomial method. Furthermore, Fathi & Sadeghi. (2022) improved the ANN method used to calibrate FHP measurements. The difference is the experimental data used in that research is only at a speed of 10 m/s. In that research, different results were found regarding the more optimal ANN method. The ANN model using the Radial Basis Function (RBF) network outperforms the MLP network used by Nikpey Somehsaraei et al. (2020). The selection of test data that is different from the training data is also a difference in the methods used by Nikpey Somehsaraei et al. (2020) and Fathi & Sadeghi. (2022). Apart from that, they both looked at the model's interpolation capabilities in the intermediate region compared to conventional methods. It was found that ANN produces better results than conventional methods which have oscillations in the intermediate region.

A different approach was taken by Zhou et al. (2023) who applied the K-nearest neighbors (KNN) algorithm in seven-hole probe measurements to measure the angle of attack on a wind turbine blade. KNN is a machine learning algorithm in the Scikit-learn library. Then Wu et al. (2022) used an estimation method based on modern ANN proposed to estimate airflow data including AoA, AoS, and air speed from pressure data at large AoA. In addition, a distributed AoA estimation ANN structure is proposed to improve the accuracy by differentiating the range of AoA. Li et al. (2023) also uses the ANN method to transform pressure data measured from FHP into flow parameters in a tail sitter VTOL UAV. They used a backpropagation-based ANN with 4 hidden layers with a variety of neurons in each layer. The model produces one output that represents AoA or AoS or velocity of the incoming flow. Multiple single-output neural networks were selected based on comparative experiments.

While sharing similarities with the research conducted by Nikpey Somehsaraei et al. (2020) and Fathi & Sadeghi. (2022), this study distinguishes itself through the utilization of input data directly derived from measured pressure data, without undergoing conversion into pressure coefficients. This approach enables the conversion of pressure measurements into parameters such as AoA, AoS, and speed directly on board the aircraft or Unmanned Aerial Vehicle (UAV). Notably, variations in speed within the measurement data differ between the two studies. In this investigation, six speed variations are considered, in contrast to the work by Fathi and Sadeghi. (2022), which focuses solely on a single speed. The tool employed for constructing the ANN model is TensorFlow, an open-source ANN library developed by Google specifically for numerical computing and machine learning applications.

1.2. Problem Definition

This Problem Definition aims to articulate the research quandary addressed through the application of ANN techniques in flow measurements. Two pivotal research inquiries guide this investigation:

1. Characteristics of ANN Models for Predicting Pressure Relationships: The primary research question delves into the characteristics of the ANN model regarding its ability to predict the relationship between pressure and velocity variables—angle α and angle β—relative to other methodologies. The emphasis is on discerning the ANN model's capacity to effectively model the correlation between pressure and these variables.
2. Effect of Hyperparameters on Prediction Accuracy: The second research question explores the impact of hyperparameters within the ANN model on the prediction accuracy of velocity variables, angle α, and angle β. The research endeavors to scrutinize various hyperparameter configurations to ascertain the optimal combination of values, thereby enhancing the prediction accuracy of the ANN model.

The research objectives encompass:

1. Comparison of existing FHP pressure data calibration methods with the proposed methodology in this study. This comparative analysis aims to unveil the advantages and disadvantages associated with each calibration method.
2. Exploration of hyperparameter combinations that minimize the prediction error of the ANN model, with the goal of improving model accuracy and optimizing prediction performance.

The research imposes specific limitations:

1. Utilization of FHP pressure data from Arifianto & Farhood. (2015) as the primary dataset.
2. Implementation of the ANN model using the Python programming language.
3. Restriction of the α angle data processing range from -20° to +20°.
4. Limitation of the β angle data processing range from -20° to +20°.
5. Use of pressure data encompassing speeds of 200, 400, 600, 800, 1000, and 1180 rpm to ensure sufficient variability in the study.

1.3. Method

In this chapter, we will elucidate the process, commencing with the utilization of FHP pressure data and culminating in the presentation of the proposed ANN model. The primary objective of this model is to forecast pressure data for the variables angle α, angle β, and speed. In this research too, conventional techniques, namely rational functions, will be used to estimate the parameter values as a comparison to the ANN model.

1.3.1. FHP Pressure Data

Pressure data derived from Arifianto & Farhood. (2015) was acquired using a custom-manufactured probe characterized by a length of 203.2 mm and a tip diameter of 5.56 mm. Each of the five holes possesses an outer diameter of 1.60 mm and an inner diameter of 0.89 mm, resulting in a hole diameter-to-tip diameter ratio of 0.16. The conical design of the probe tip features a 90° angle, facilitating precise measurements of the α angle and β angle at low speeds. Furthermore, the probe can be calibrated to accurately measure these angles within the range of ±22.5°.

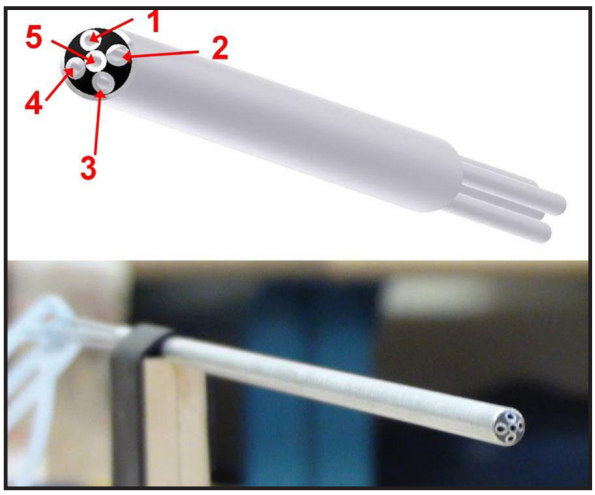

Figure 2-1 Five-hole pressure probe(Arifianto & Farhood, 2015a)

Probe calibration was executed at the Subsonic Open Jet Wind Tunnel located at Virginia Tech. The calibration procedure involved incrementally increasing the speed of the wind tunnel fan from 200 to 1180 rpm, with increments of 200 rpm. At each speed, the angles α and β were systematically varied within the range of -20° to +20°, with increments of 5°. Thus, with 6 variations of speed, 9 variations of angle α, and 9 variations of angle β, resulting in a total acquisition of 486 data points.

This set of 486 pressure data points will be utilized in the present research, employing the ANN approach to discern and predict the intricate relationship between pressure and the variables angle α, angle β, and speed. Each individual data point represents the pressure data corresponding to specific values of angle α, angle β, and speed. Figure 2-2 illustrates the pressure measurements for diverse angles α and β at a fan speed of 600 rpm.

1.3.2 Data Preparation

For this research, two methodologies were employed to select training and validation data. The ratio of the amount of data for training and validation in an ANN can vary depending on the total size of the dataset and the specific characteristics of the problem at hand. Generally, the data split is 70-80% for training data and 20-30% for validation data. If the size of the data set is large (for example up to millions), the proportion for validation data can be smaller because the absolute size is still sufficient.

In the initial approach, data was randomly partitioned, with 80% allocated to training and 20% to validation. As depicted in Figure 2-3 and Figure 2-4, the histogram illustrates a well-distributed dataset. However, certain validation data points, such as P1 and P4, still fall outside the training data distribution.

In the second data selection method, the training data contains all the outer data points (pressure data at angles α at -20° and 20°, angles β at -20° and 20°) at all speeds. All these outermost data points totaled 192. To fulfill 80% of the training data from the data set (i.e. 388 data points), then 196 data points were randomly selected from the remaining data set. Histograms of training and validation data using this method are presented in Figure 2-5 and Figure 2-6.

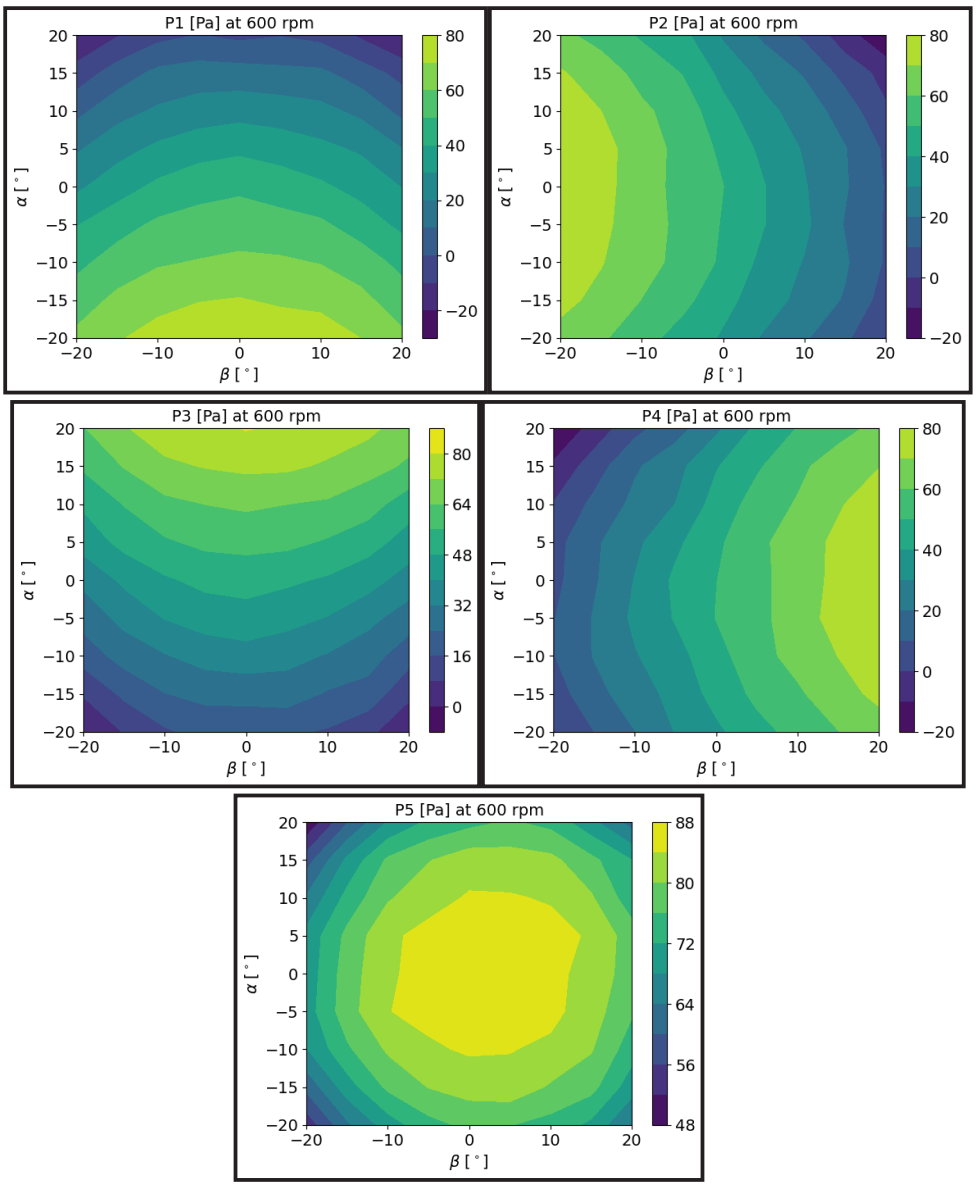

Figure 2-2 Pressure distribution at various configurations of angle values α and β for each probe hole

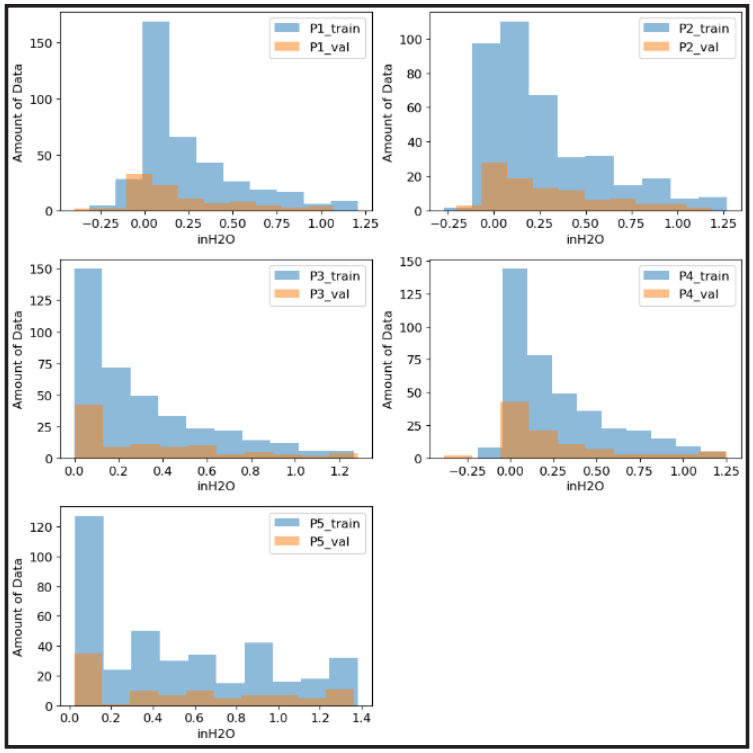

Figure 2-3 Histogram of Train data vs Validation data as input method 1

When employing the second method, all validation data points fall within the range of the training data. This outcome aligns with expectations, as ANN excels at interpolation. Consequently, the second data selection method is anticipated to yield an ANN model that more accurately approximates the relationships among variables compared to the first method.

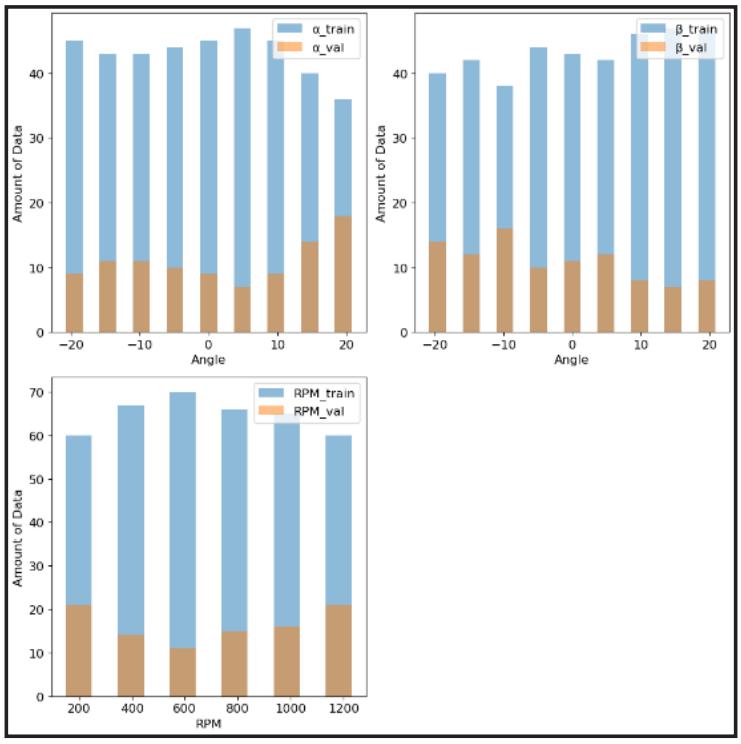

Figure 2-4 Histogram of Train data vs Validation data as the output of method 1

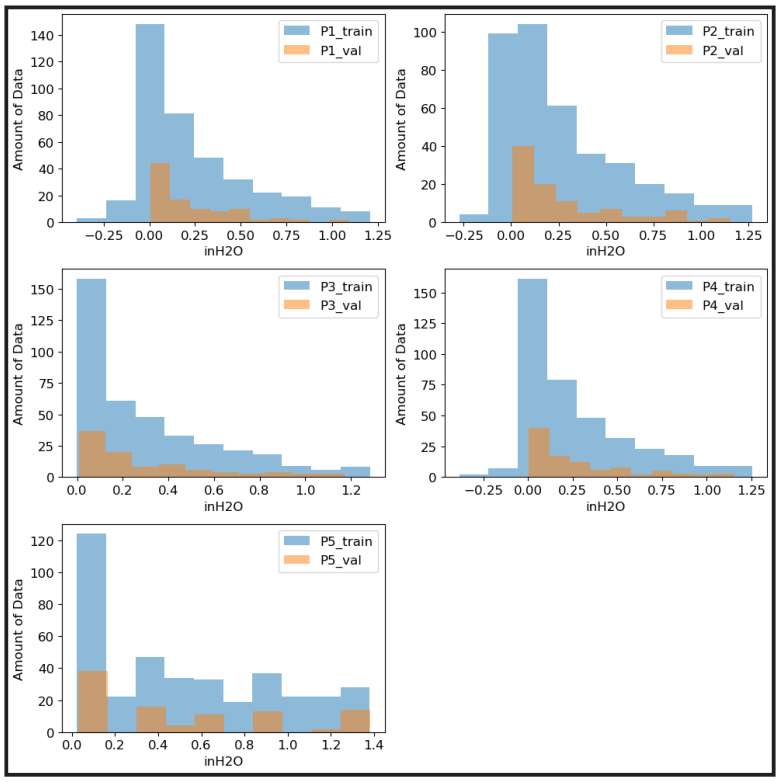

Figure 2-5 Histogram of Train data vs Validation data as input of method 2

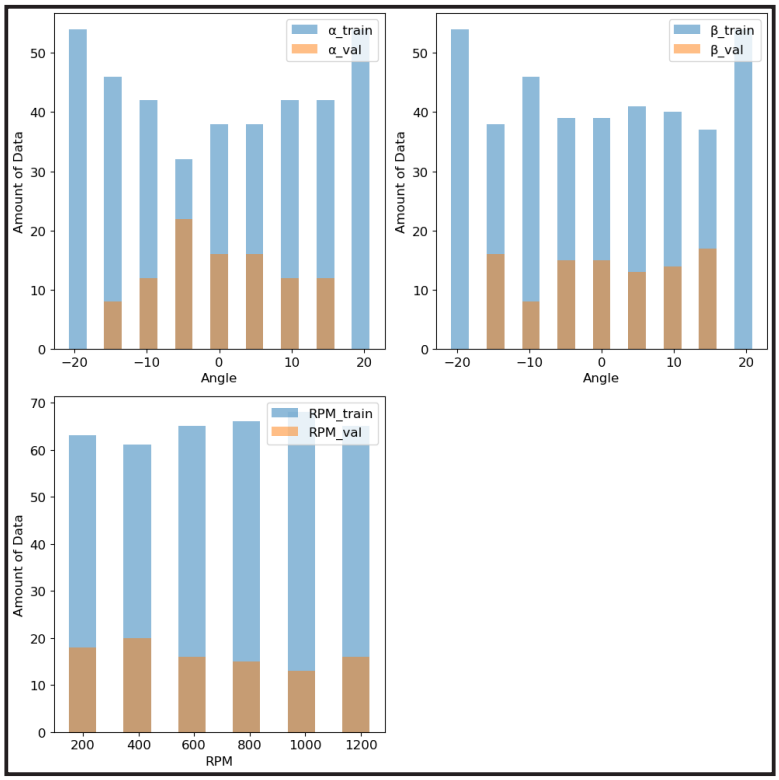

Figure 2-6 Histogram of Train data vs Validation data as output of method 2

1.3.3. ANN Modeling

This study meticulously followed a series of steps, as delineated in Figure 2-7, to construct an optimized ANN model. A systematic test was conducted to assess the impact of training data selection on model accuracy. To further enhance accuracy, optimal combinations of hyperparameters were identified through multiple trials. These trials encompassed adjustments such as increasing the number of neurons, selecting an optimal activation function and optimizer, and introducing hidden layers to observe their impact on loss and accuracy.

In the initial step, our model incorporated one hidden layer with 16 neurons, employing the SeLU activation function and Adam optimizer. The MAE was utilized as the loss function, with its values monitored throughout the training process. To assess the model's performance, both method 1 and method 2 were applied to the training data. The efficacy of each model was gauged based on the estimation results for both the training and validation data.

Upon analyzing the preliminary test results, it was discerned that method 2 resulted in a smaller loss compared to method 1. Consequently, method 2 data selection was chosen for the subsequent refinement of the ANN model. The outcomes of this test are presented in Table 2-1.

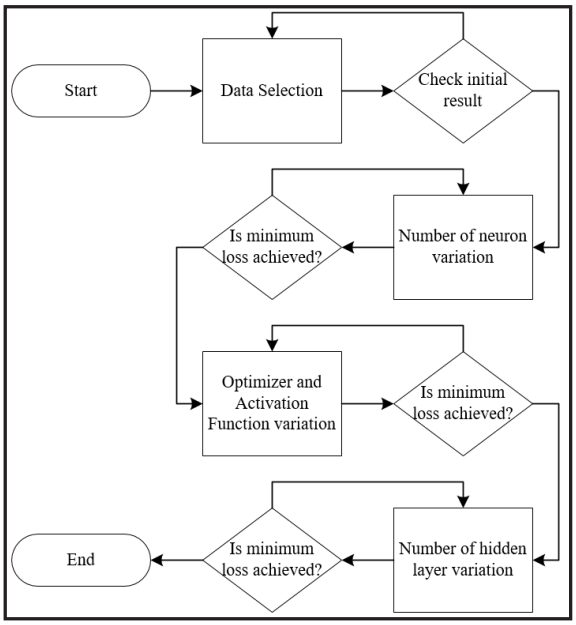

Figure 2-7 Flowchart ANN modeling

Table 2-1: Comparison of the initial result between different methods of data selection

Method	Statistical parameter	α	β	RPM
Method 1	MAE	5.73502	5.94318	35.4984
	Max AERR	19.1146	19.1867	251.476
	R2	0.65117	0.62600	0.97675
Method 2	MAE	5.52152	5.93043	36.9209
	Max AERR	20.7831	19.2126	213.027
	R2	0.67163	0.62423	0.97645

In the subsequent phase, neurons are incrementally added to the model, with the number of neurons spanning from 16 to 100. As depicted in Figure 2-8, the minimum loss is attained when the model incorporates 97 neurons. This value has been identified as the optimal number for constructing the ANN model.

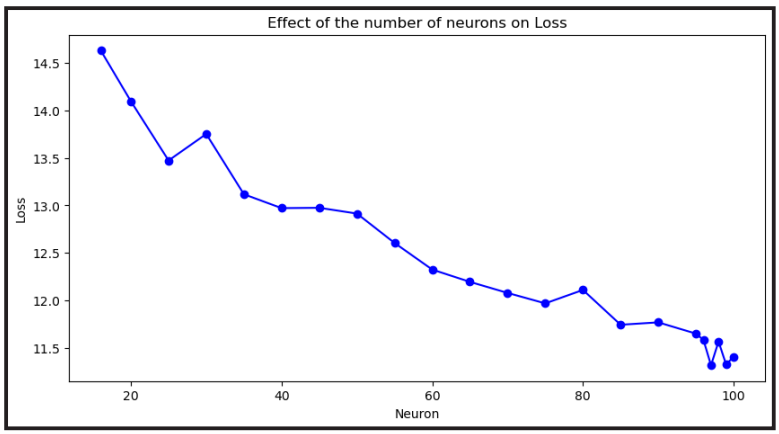

Figure 2-8 Number of neurons variation

Following the determination of the optimal number of neurons, a series of tests were conducted on various activation and optimizer functions. The activation functions examined encompassed ReLU, Sigmoid, tanh, Softplus, Softsign, SeLU, eLU, and exponential. Simultaneously, the optimizer functions tested included Adam, Rmsprop, SGD, Adadelta, Adagrad, Adamax, Nadam, and FTRL. The exploration of these activation and optimizer function variations resulted in a total of 64 combinations of ANN structures.

Based on the outcomes illustrated in Figure 2-9, it was observed that utilizing the combination of Adam as the optimizer and SeLU as the activation function yielded the smallest loss value, registering at 1.69.

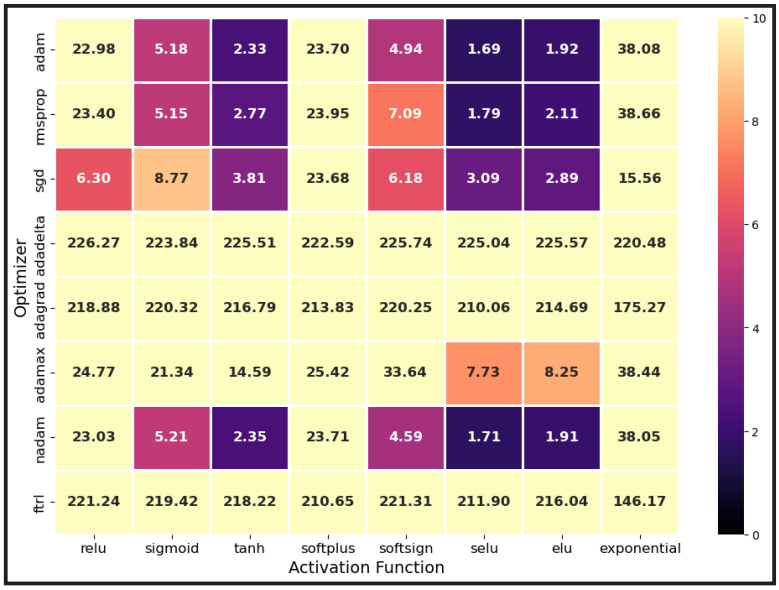

Figure 2-9 Activation function and Optimizer variation

Multiple trials were carried out to assess the influence of hidden layers on the outcomes, ranging from 1 to 6 hidden layers. The data depicted in Figure 2-10 clearly indicates that utilizing 4 hidden layers can contribute to a noteworthy reduction in loss. However, a further increase in the number of hidden layers may lead to a higher loss value, signifying a potential issue of overfitting.

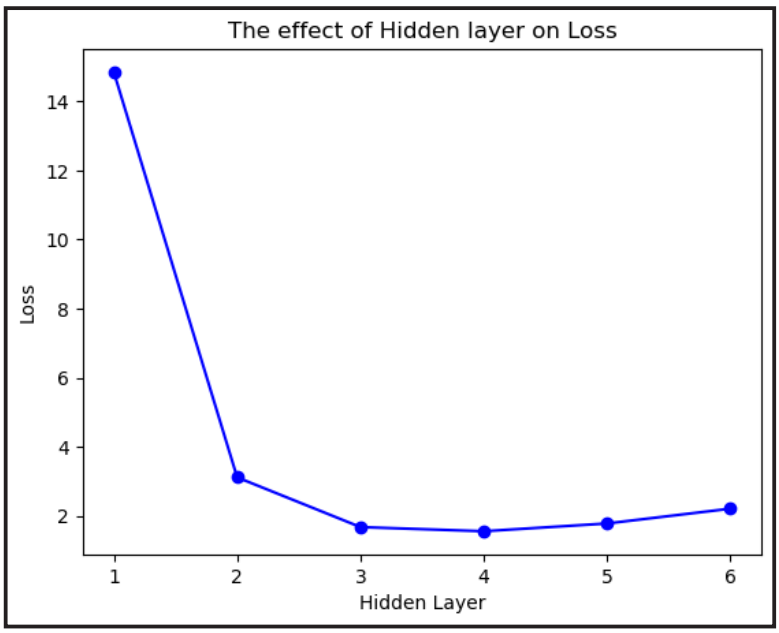

Figure 2-10 Hidden layer variation

1.3.4. Rational function

In this technique as used in Arifianto & Farhood. (2015), equations (2-1) are used to calculate angle α and angle β from the FHP pressure data. The coefficients $a_0, a_1, \ldots\ldots, a_8$ and $b_0, b_1, \ldots\ldots, b_{10}$ are obtained by solving the least-squares problem with linear regression. The equations are defined as:

$$\alpha = \frac{a_0 + a_1 C_{p\alpha} + a_2 C_{p\beta} + a_3 C_{p\beta}^2 + a_4 C_{p\beta}^3}{1 + a_5 C_{p\alpha} + a_6 C_{p\beta} + a_7 C_{p\beta}^2 + a_8 C_{p\beta}^3}$$

$$\beta = \frac{b_0 + b_1 C_{p\alpha} + b_2 C_{p\beta} + b_3 C_{p\alpha}^2 + b_4 C_{p\beta}^2 + b_5 C_{p\alpha} C_{p\beta}}{1 + b_6 C_{p\alpha} + b_7 C_{p\beta} + b_8 C_{p\alpha}^2 + b_9 C_{p\beta}^2 + b_{10} C_{p\alpha} C_{p\beta}}$$

where,

$$C_{P_\alpha} = \frac{P_3 - P_1}{P_5 - \bar{P}};\ C_{P_\beta} = \frac{P_4 - P_2}{P_5 - \bar{P}};$$

$$\bar{P} = 0.25(P1 + P2 + P3 + P4) \qquad (2-1)$$

Solving the least-squares problem with linear regression involves finding the coefficients that minimize the sum of the squared differences between the predicted and actual values of the target variable. Linear regression is a statistical method used for modeling the relationship between a dependent variable (target) and one or more independent variables (features) by fitting a linear equation to observed data.

Equation (2-1) can then be expressed as follows:

$$\alpha = a_0 + a_1 C_{p\alpha} + a_2 C_{p\beta} + a_3 C_{p\beta}^2 + a_4 C_{p\beta}^3$$

$$\beta = b_0 + b_1 C_{p\alpha} + b_2 C_{p\beta} + b_3 C_{p\alpha}^2 + b_4 C_{p\beta}^2 + b_5 C_{p\alpha} C_{p\beta} - b_6 C_{p\alpha}\beta - b_7 C_{p\beta}\beta - b_8 C_{p\alpha}^2\beta - b_9 C_{p\beta}^2\beta - b_{10} C_{p\alpha} C_{p\beta}\beta \qquad (2-2)$$

Equation (2-2) is shortened to matrix format as:

$$[Y] = [k][X] \qquad (2-3)$$

where Y is a matrix containing one of the flow parameters, k is a matrix containing rational function constants, and X is a matrix containing pressure coefficients. The YY matrix is determined by the flow characteristics measured in the wind tunnel. Therefore, the estimation of unknown coefficients of rational functions is the goal of this calibration method. The coefficients of rational function is calculated as:

$$[k] = [X^T X]^{-1}[X]^T[Y] \quad (2-4)$$

The calibration procedure was finished once the coefficients of rational function converged. The coefficient values obtained for $\alpha\alpha$ and $\beta\beta$ are shown in the Table 2-2.

Table 2-2: coefficient values of rational functions

Coefficient	Value	Coefficient	Value
a_0	-1.7989	b_0	-0.2091
a_1	11.0255	b_1	0.0400
a_2	0.0925	b_2	-11.0124
a_3	-0.1106	b_3	0.0975
a_4	-0.0045	b_4	-0.6957
a_5	-0.0103	b_5	-0.3676
a_6	0.0395	b_6	0.0328
a_7	0.0528	b_7	0.1261
a_8	0.0005	b_8	0.0367
		b_9	0.0275
		b_{10}	0.0035

2. Result and Analysis

This chapter aims to compare the ANN model's performance with other existing techniques. The technique being compared is the rational function technique used by Arifianto & Farhood. (2015). Three primary parameters, namely the coefficient of determination (r^2), mean absolute error (MAE), and maximum absolute error (Max AERR), were utilized to evaluate and compare the performance of the developed ANN. They are defined as follows:

$$MAE = \frac{\sum_{i=1}^{N}|\hat{y}_i - y_i|}{N} \quad (3-1)$$

$$r^2 = 1 - \frac{\sum_{i=1}^{N}(\hat{y}_i - y_i)^2}{\sum_{i=1}^{N}(\hat{y}_i - \bar{y})^2} \quad (3-2)$$

$$Max\ AERR = \max(|\hat{y}_i - y_i|) \quad (3-3)$$

where $\hat{y}_i$, y_i , and $\bar{y}$ represent the *i*-th approximated, *i*-th measured, and the average of measured values respectively. *N* denotes the number of samples.

By employing the rational function, r^2 values of 0.9949 and 0.9972 were attained for α and β, respectively. In contrast, leveraging the ANN technique yielded r^2 values of 0.99925, 0.99893, and 0.99998 for α, β, and speed, respectively. The notably high r^2 values signify an excellent correspondence between predicted and measured values. This is visually demonstrated in Figure 3-1, where the x and y axes represent the desired values for α and β. The predicted result is exactly near the desired value.

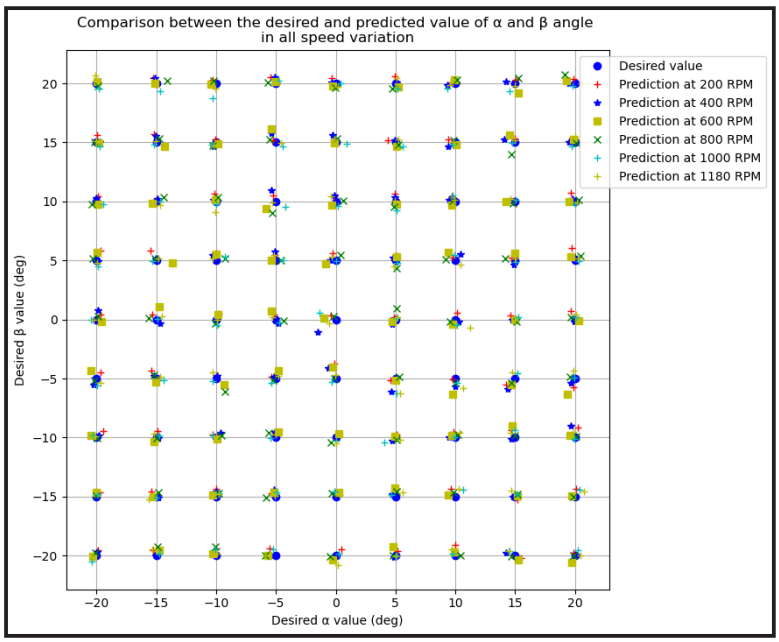

Figure 3-1 Comparison between the desired and predicted values of α and β

In order to evaluate the prediction accuracy of each technique, we will use statistical parameters such as MAE, Max AERR, and r^2. You can view the comparison results in Table 3-1.

Table 3-1: Comparison of calibration results based on ANN and Rational function

Method	Statistical parameter	α	β	RPM
Rational Function	MAE	0.76701	0.54421	-
	Max AERR	4.255	1.9846	-
	r^2	0.99426	0.99734	-
ANN	MAE	0.27050	0.33260	1.07475
	Max AERR	1.52825	1.31180	7.21741
	r^2	0.99925	0.99893	0.99998

The table above shows that the ANN technique with the proposed model produces better approximation performance than the rational function. One factor that may improve the modeling process is using ANN to directly process the raw pressure data based on α, β, and speed. This approach eliminates errors that may occur when converting the pressure data into a pressure coefficient, as is typically done with the rational function.

It's important to keep in mind that creating an ANN model can be time-consuming, especially when dealing with large amounts of data. Numerous iterations are necessary, which can pose a challenge. For instance, determining the optimal number of neurons in a single iteration can take up to four hours. This process is repeated for each subsequent search for optimal hyperparameters.

3. Conclusions

Based on the conducted research and the comparative analysis of approximation results between the ANN and rational function techniques, the following conclusions can be drawn:

1. The ANN technique demonstrates superior accuracy compared to the rational function technique for the provided pressure data. The coefficient of determination for the ANN technique stands at 0.99925 and 0.99893 for angles α and β, respectively, while the rational function technique yields r^2 values of 0.99426 and 0.99734 for angles α and β.
2. The implementation of the ANN technique resulted in a noteworthy improvement, with a 64.7% reduction in MAE values for angle α and a 38.9% reduction for angle β when compared to the rational function technique.

3. The optimal structure of the ANN model comprises four hidden layers with the following number of neurons in each layer: [97, 100, 97, 100]. The SeLu activation function and Adam optimizer are employed for optimal performance.

Contributorship Statement

AB is the main contributor. OA and TM are advisors.

References

Arifianto, O., & Farhood, M. (2015a). Development and Modeling of a Low-Cost Unmanned Aerial Vehicle Research Platform. *Journal of Intelligent and Robotic Systems: Theory and Applications*, *80*(1), 139–164. https://doi.org/10.1007/s10846-014-0145-3

Arifianto, O., & Farhood, M. (2015b). Development and Modeling of a Low-Cost Unmanned Aerial Vehicle Research Platform. *Journal of Intelligent and Robotic Systems: Theory and Applications*, *80*(1), 139–164. https://doi.org/10.1007/s10846-014-0145-3

Fathi, S., & Sadeghi, H. (2022). Improvement of the five-hole probe calibration using artificial neural networks. *Flow Measurement and Instrumentation*, *86*. https://doi.org/10.1016/j.flowmeasinst.2022.102189

Gallington, R. (1980). *Measurement of Very Large Flow Angles with Non-nulling Seven- Hole Probes*.

Li, X., Wu, Y., Shan, X., Zhang, H., & Chen, Y. (2023). Estimation of Airflow Parameters for Tail-Sitter UAV through a 5-Hole Probe Based on an ANN. *Sensors*, *23*(1). https://doi.org/10.3390/s23010417

Liu, J. (2023). The angle of attack and side-slip angle estimation for civil aircraft. *Journal of Physics: Conference Series*, *2569*(1). https://doi.org/10.1088/1742-6596/2569/1/012072

Mortadha, J., & Qureshi, I. (2019). Extending the usable range of the calibration map of a four-hole probe for measuring high flow angles. *Flow Measurement and Instrumentation*, *65*, 257–267. https://doi.org/10.1016/j.flowmeasinst.2019.01.013

Nikpey Somehsaraei, H., Hölle, M., Hönen, H., & Assadi, M. (2020). A novel approach based on artificial neural network for calibration of multi-hole pressure probes. *Flow Measurement and Instrumentation*, *73*. https://doi.org/10.1016/j.flowmeasinst.2020.101739

Pisasale, A. J., & Ahmed, N. A. (2002). A novel method for extending the calibration range of five-hole probe for highly three-dimensional flows. In *Flow Measurement and Instrumentation* (Vol. 13). www.elsevier.com/locate/flowmeasinst

Popowski, S., & Dabrowski, W. (2015). Measurement and estimation of the angle of attack and the angle of sideslip. *Aviation*, *19*(1), 19–24. https://doi.org/10.3846/16487788.2015.1015293

Ranjan Paul, A., Ranjan Upadhyay, R., & Jain, A. (2011). A novel calibration algorithm for five-hole pressure probe. In *International Journal of Engineering, Science and Technology* (Vol. 3, Issue 2). www.ijest-ng.com

Treaster, A. L., & Yocum, A. M. (1978). *THE CALIBRATION AND APPLICATION OF FIVE-HOLE PROBES*.

Wu, X., Li, X., Shan, & Y, C. (2022). Evaluation and Improvement of Five-hole Pressure Probe's Performance at Large AOA based on ANN. *AIAA AVIATION 2022 Forum*.

Zhou, S., Wu, G., Dong, Y., Ni, Y., Hao, Y., Jiang, Y., Zhou, C., & Tao, Z. (2023). Evaluations on supervised learning methods in the calibration of seven-hole pressure probes. *PLoS ONE*, *18*(1 January). https://doi.org/10.1371/journal.pone.0277672